Numerical Analysis of Void-Induced Thermal Effects on GaAs/AlGaAs High Power Quantum Well Laser Diodes

F. Gity[1,2], V. Ahmadi[1,2], M. Noshiravani[2], and K. Abedi[1,3]

1. Dept. of Electrical Engineering, Tarbiat Modares University, Tehran, Iran, P. O. Box: 14115-143
2. Laser Research Center, AEOI, P. O. BOX: 14155-1339
3. Islamic Azad University, Ahar Branch

Corresponding author: v_ahmadi@modares.ac.ir

***Abstract* — Microscopic voids in the die attachment solder layers of high power laser diodes (HPLDs) cause to degrade their overall thermal transfer performance. This paper presents the effects of voids on the thermal conductivity, leakage and threshold currents, characteristic temperature (T_0) and output power of a single quantum well (SQW) HPLD. These effects are modeled by means of finite difference method (FDM). This numerical model calculates the time-dependent axial variations of photon density, carrier density and temperature in semiconductor laser self-consistently. The temperature dependence of the wavelength shift and the thermal mode hopping concept is also demonstrated.**

***Index Terms* — finite difference method, hot spot, high power laser diode, mode hopping, thermal behavior, thermal rollover, void, wavelength shift.**

I. Introduction

High power semiconductor laser diodes and power amplifiers play important roles in solid state laser and optical fiber pumping, optical storage and recording, and can serve as efficient sources for medical and direct material applications [1]. The performance of the laser is highly dependent upon the temperature of the active region. These high power devices must be mounted in the epitaxy-side down configuration for good heat transfer and so require a well controlled, high yield, void-free die attach interface. Lifetime of HPLDs is sensitively related to operating temperature, mounting stress and solder voids. These voids reduce the ability of the die-attach solder layer to conduct heat from the laser to the heat sink. Increasing the optical output power has been the trend for semiconductor laser development, e.g., in recent years, the operating power of pump lasers has roughly doubled every two years [2]. However, the reliability and efficiency of a high-power laser are hampered by the nonlinear temperature. This nonlinear temperature is caused by high intensity laser light. Thus, thermal management of high power lasers is critical since the junction temperature rise that results from large heat fluxes strongly affects the device characteristics [3]. The chip and package structure must provide efficient heat transfer from the active region to the heat sink and should not produce excessive stress on the laser diode. The absorption and subsequent nonradiative recombination of laser light increase the operating temperature of the laser. The temperature of the active region has been observed to be significantly higher than that of the heat sink during lasing, and therefore catastrophic optical damage (COD) occurs. Several analytical and numerical models have been developed to estimate the carrier density, photon density and temperature along the laser cavity. The calculations are based on the finite element method [4], beam propagation method [5] and transmission line matrix method [6]. In [7], thermal runaway in the AlGaAs double-heterostructure laser is studied. The authors solved the one-dimensional stationary carrier diffusion equation analytically and gave an estimation of the temperature rise in the facet region without considering voided area effects. In [8], a comprehensive three-dimensional thermal model was used to calculate the time dependent temperature distribution at the laser diode facets. However, the heat conduction was not coupled to the carrier and photon densities. An analytical solution of the three-dimensional heat conduction equation and a one-dimensional carrier diffusion equation is used in [9].

In this paper a GaAs/AlGaAs SQW HPLD is modeled by FDM using an exact gain function. The model calculates self-consistently the time dependent axial variation of photon density, carrier density and temperature through solving the rate equations of photon and carrier densities coupled with the heat conduction equation including void effects. We have incorporated different parameters that have remarkable influence on the thermal behavior of a HPLD.

In section II we have described the physics and theory of the model. Numerical results and discussion about thermal induced effects inside the cavity, thermal mode hopping and void-induced thermal effects on optical and electrical characteristics of the laser are included in section III. Finally in section IV a conclusion is presented.

II. PHYSICS AND THEORY OF THE MODEL

A. Model

A SQW Fabry-Perot GaAs/AlGaAs HPLD is considered. The model starts with the rate equations for the photon densities of the forward (S^+) and backward (S^-) running wave:

$$\frac{\partial S^+}{\partial t}+v_g\frac{\partial S^+}{\partial z}=v_g\left[\Gamma g(E,n,T)-\alpha_{tot}(n)\right]S^+ +10^{-4}B_{sp}(T)n^2 \tag{1}$$

$$\frac{\partial S^-}{\partial t}-v_g\frac{\partial S^-}{\partial z}=v_g\left[\Gamma g(E,n,T)-\alpha_{tot}(n)\right]S^- +10^{-4}B_{sp}(T)n^2 \tag{2}$$

where $g(E,n,T)$ is the gain and α_{tot} is the total optical loss and B_{sp} is the function describing the temperature dependence of the spontaneous emission. In (1) and (2) and in the following equations, t is the time and z is the axial coordinate (z = 0-L). Full parameters of our model are listed in table I.

In order to calculate the carrier diffusion within the resonator, the following nonlinear ambipolar diffusion equation is considered:

$$\frac{\partial n}{\partial t}=D\frac{\partial^2 n}{\partial z^2}+\frac{J(z)}{qL_z}-v_g\left[g(E,n,T)-\sigma_{fc}n\right]\times\left[S^+ +S^-\right]-\frac{n}{\tau_e(n,T)} \tag{3}$$

here, *J(z)* is the injection current density.

To involve thermal effects, (1) to (3) should be solved coupled with the heat conduction equation:

$$\rho_m c_p\frac{\partial T}{\partial t}=k_z\frac{\partial^2 T}{\partial z^2}+q(n,T)-\gamma\left[T-T_{hs}\right]. \tag{4}$$

The function *q(n,T)* describes the power density of the heat production within the active region. The last term shows the thermal interaction of the laser and the heat sink.

Experimental measurements [10] and also numerical models [11]-[12] for devices with various levels of die-attach voids show that large-area die-attach defects (voids) increase the thermal impedance of high power semiconductor devices. This data is then correlated with finite deference thermal modeling to improve the estimation of peak die temperature for voided HPLDs. We defined γ from the experimental results as follows:

$$\gamma=-0.054/\left(1+\exp\left(-\left(VP-15\right)/4.2\right)\right)+0.055 \tag{5}$$

In (5) and other parts of this paper, *VP* stands for the voided area percentage.

The energy of the photons in (1) to (3) is determined by the maximum of the gain curve. This maximum is determined by the separation energy, E_q, of the ground levels of the conduction and valance bands (bandgap). For modeling the thermal bandgap shrinkage the expression given in [13] is used:

$$E_q(T)=\left[E_0-\frac{5.405\times10^{-4}\times T^2}{T+204}\right] \tag{6}$$

The above system of nonlinear partial deferential equations represents a combined initial value/boundary value problem. The boundary values for the photon density arise from the reflection of the waves at the facets:

$$\begin{aligned}S^+(0,t)&=R_0S^-(0,t)\\ S^-(L,t)&=R_LS^+(L,t).\end{aligned} \tag{7}$$

It is common practice to assume that the carriers recombine at the facets with a typical recombination velocity. This is mathematically expressed as:

$$\begin{aligned}-D\frac{\partial n}{\partial z}(0,t)&=-v_0n(0,t)\\ -D\frac{\partial n}{\partial z}(L,t)&=+v_Ln(L,t).\end{aligned} \tag{8}$$

It is assumed that the recombination of every electron-hole pair frees an amount of heat, which corresponds to their energetic separation E_q. The heat flux density at the facets is proportional to the production of E_q and the amount of recombination events per unit time per unit area, v_0n and v_Ln:

$$\begin{aligned}-k_z\frac{\partial T}{\partial z}(0,t)&=+E_q\left[T(0,t)\right]v_0n(0,t)\\ -k_z\frac{\partial T}{\partial z}(L,t)&=-E_q\left[T(L,t)\right]v_Ln(L,t).\end{aligned} \tag{9}$$

B. Numerical treatment

In this model the effects of spontaneous emission, Auger recombination, carrier lifetime and temperature induced bandgap shrinkage are included.

For numerical treatment (1) to (9) are written in dimensionless form by introduction of the new independent variables $\xi=z/L$ and $\tau=t/\tau_0$. We have assumed that $\tau_0=1\,ns$ and $L=600\mu m$, also $L_z=100\,^\circ A$ and $\Delta E_c/\Delta E_v=0.6/0.4$ The dependent variables are $\sigma^+=S^+/S_0$, $\sigma^-=S^-/S_0$, $\nu=n/n_0$ and $\theta=T/T_{hs}$. To let the variables be order of one, $S_0=10^{14}cm^{-3}$ and $n_0=10^{18}cm^{-3}$ were chosen.

The system of coupled nonlinear partial deferential equations is solved by the FDM, and the course/fine structure of element size was applied to this method in order to get an exact profile near the facets.

In order to apply thermal effects more precisely, exact gain calculations must be used rather than approximate gain calculations. So, to reach exact results of void-induced thermal effects we have made use of Fermi's golden rule in our model, as follows [14]:

$$g(E,n,T) = g_0|M|^2 \times \rho_{red}/E \times \left(f_c(E,n,T) + f_v(E,n,T) - 1\right) \qquad (10)$$
$$g_0 = q^2\hbar\pi/\varepsilon_0 m_0^2 c_0 n$$

Spectral broadening lowers the calculated peak gain and shifts the calculated emission wavelength of the laser to a shorter wavelength. It is phenomenologically included through a Lorentzian-shaped broadening function:

$$G(E,n,T) = \int_0^\infty g(W,n,T)\frac{(1/\pi)(\hbar/\tau_{in})dW}{(\hbar/\tau_{in})^2 + (W-E)^2}. \qquad (11)$$

Beside the thermal shrinkage of the bandgap, the carrier-induced renormalization of the bandgap has also been included through the following relation [15]:

$$\Delta E_g(n_s) = -10^{-3}\left(n_s/cm^{-2}\right)^{1/3} \qquad (12)$$

where n_s is the sheet carrier density.

The total optical loss in (1) and (2) reads as [16]:

$$\alpha_{tot}(n) = \alpha_m + \alpha_{sc} + \Gamma\sigma_{fc}n. \qquad (13)$$

Based on the comparison made with [17], the following expression was used to determine the spontaneous emission rate:

$$B_{sp}(T) = 1.7\times10^{-16}\frac{300}{T}. \qquad (14)$$

The carrier lifetime is determined by spontaneous emission, interface recombination and Auger recombination as follows [16]:

$$\tau_e(n,T) = \left[A_{nr} + B_{sp}(T)n + C_{aug}(T)n^2\right]^{-1} \qquad (15)$$

where

$$C_{aug}(T) = 4.2\times10^{-42}\exp\left(\frac{T_A}{300} - \frac{T_A}{T}\right)\sqrt{\frac{T}{T_A}} \qquad (16)$$

is the Auger recombination coefficient. The characteristic temperature T_A describes the temperature dependence of Auger recombination phenominologically [15]. The power density of heat produced in the resonator is proportional to the Auger recombination rate and the energy difference of the recombining particles (E_q). Thus, it can be written as follows:

$$q(n,T) = E_q(T)C_{aug}(T)n^3. \qquad (17)$$

Lasing occurs when the carrier density within the active region is high enough to result in a peak gain that equals the losses. This is mathematically expressed as follows [16]:

$$\Gamma g_{\max}(n_{th},T) = \alpha_{tot}(n_{th}). \qquad (18)$$

By solving this nonlinear equation the temperature dependence threshold carrier density is obtained.

At threshold stimulated emission can be ignored and the carrier density is clamped to its threshold value. So the threshold current density can be reached through the following equation [16]:

$$J_{th}(T) = \frac{qL_z n_{th}(T)}{\tau_e(n_{th},T)} \qquad (19)$$

Table I. Parameters used in the model

Symbol	Description
v_g	Group velocity of light
D	Diffusion constant in the active region
c_p, k_z, ρ_m	Specific heat capacitance, thermal conductivity and mass density of the resonator material
α_m, α_{sc}	Mirror and scattering loss
L_z,L	Quantum well thickness and the cavity length
T_{hs}	Heat sink temperature
R_0,R_L	Intensity reflection coefficients
A_{nr}	Coefficient of interface recombination
T_A	Characteristic temperature for Auger recombination
γ	Balance coefficient between laser and heat sink
Γ	Confinement factor
τ_{in}	Interaband relaxation time
σ_{fc}	Free carrier absorption cross section
v_0,v_L	Surface recombination velocities
c_0	Velocity of light in vacuum
m_0	Electron rest mass
ε_0	Permittivity of vacuum
n	Effective index of refraction of the active region
x_p	p-cladding layer thickness
L_n	Minority electron diffusion length
σ_p	Electrical conductivity of the p-cladding layer

III. Numerical Results and Discussion

A. Thermal induced effects inside the cavity

Due to the remarkable different facet reflection coefficients, the profiles are asymmetric. The profiles of the photon density, carrier density and temperature for two different pumping currents and for 23% voided area

are represented in Fig. 1. The axial distribution of photons is shown in Fig. 1(a). The total photon density is the sum of the forward (S^+) and backward (S^-) running wave. As indicated in the figure, the photon density increases nonlinearly with pumping current. This increase is considerable at the left side of the cavity. Note that the anti-reflection- (AR-) coated mirror is on the left side. Fig. 2(b) shows the profile of carrier density in the cavity. The average carrier density increases with pumping current, but as illustrated at the left side of the Fig. 2(b), the carrier profile has the inverse relation with current. The reason is the high optical field and strong stimulated emission at the AR-coated side of the cavity, as stated before. Fig. 2(c) illustrates the axial distribution of the temperature along the cavity length. The temperature at both ends is more that the inner region since the surface recombination occurs at laser facets. The inner region of the resonator which determines the output wavelength is considerably heated by Auger recombination, according to (17). Total loss of the cavity is directly proportional to the pumping current, therefore, the temperature of the cavity is increased by current; on the other hand because of the bandgap thermal shrinkage the peak of the gain is inversely proportional to temperature, so in order to compensate these effects the carrier density along the cavity increases with current. The higher reflection coefficient at the right side of the cavity causes a greater temperature increase in that region. If the effects of thermal bandgap shrinkage and bandgap renormalization were not included in the model, the precise information given above would not have been achieved.

Another important point is the positive feedback that leads to COD. An increase in the temperature causes the bandgap to shrink, leading to absorption of photons. The photon reabsorption generates electron-hole pairs, which in turn recombine nonradiatively, thus producing extra heat. This circular process is the main reason for COD.

B. Thermal mode hopping

The most important point to be considered while analyzing HPLDs is the shift of the output wavelength from the beginning of the lasing to the steady state mode. As described above, the temperature of the resonator changes until the thermal equilibrium condition between the resonator and the heat sink is reached. Temperature dependence of the bandgap and the quasi-Fermi levels and therefore the temperature dependence of the gain relate the output wavelength to the temperature of the active region. Tracking different wavelengths during the transient time shows a great shift of λ. Fig. 2 shows this considerable process. As indicated in the figure the dominant mode of the laser at the beginning was $\lambda = 832\,nm$ while after 300 *ns* the output wavelength changes to $\lambda = 840.2\,nm$ which is in agreement with the temperature dependence of the wavelength [18].

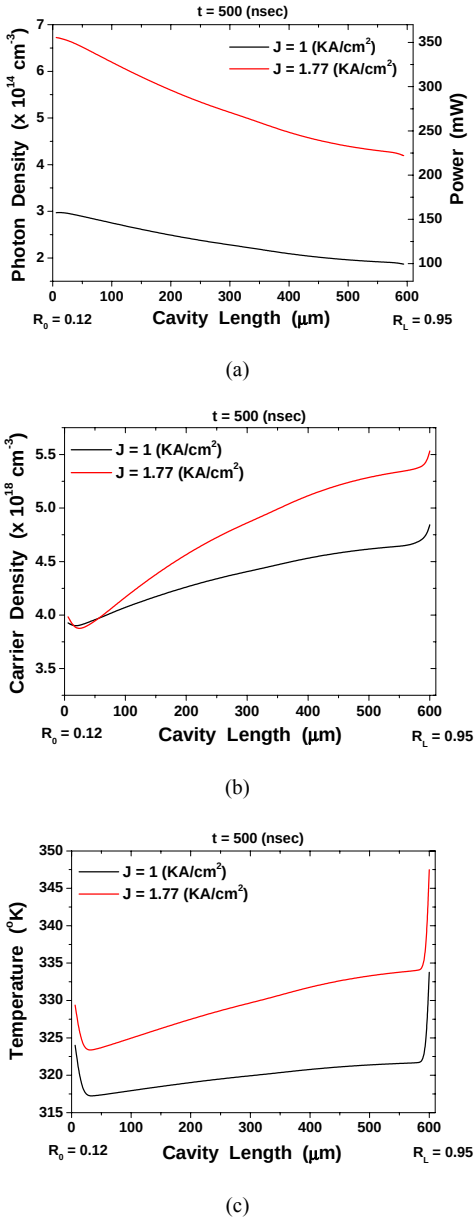

Fig. 1. Axial distributions (considering 23% voided area) of photon density, (b) carrier density, and (c) temperature (a)

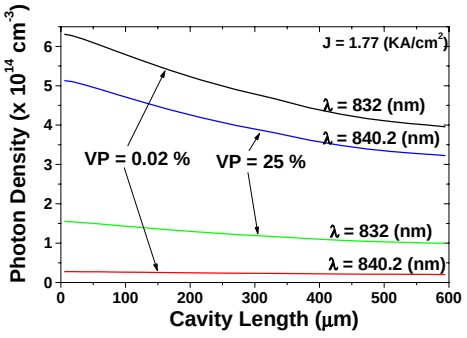

Fig. 2. Mode hopping due to thermal effects

C. Void-induced thermal effects on optical and electrical characteristics of the laser

The effects of different percentage voided areas on axial temperature profile along the cavity are shown in Fig. 3. As seen in this figure, high percentage voided areas cause a greater temperature increase at the laser facets. Therefore, the probability of the occurrence of COD becomes greater with increased percentage voided area.

The kinetic energy of those electrons located above the quasi-Fermi levels of the conduction and valance bands builds up with temperature. Thus the leakage current through the following relations will also increase with temperature [15]. On the other hand, as a result of temperature increase the peak of the gain will decrease and will also have a red shift (Fig. 4). Because of the above reasons, the threshold current density will get a higher value while the voids of the interface become larger in size and number as indicated in Fig. 5, which is in agreement with [19].

Leakage current density can be calculated as [15]:

$$J_L = qD_n N_0 [\sqrt{\frac{1}{L_n^2}+\frac{1}{4z^2}}\times \coth\sqrt{\frac{1}{L_n^2}+\frac{1}{4z^2}}\,x_P+\frac{1}{2z}] \quad (20)$$

where

$$z=\left(\frac{k_B T}{q}\right)\frac{\sigma_p}{J_{tot}} \quad , \quad J_{tot}=J_R+J_L \quad (21)$$

and N_0 is the electron concentration at the interface of the active region and the p-cladding layer. N_0 is linked to the energy separation between the quasi-Fermi level and the top of the quantum well (ΔE) through the following relation [15]:

$$N_0 = N_c.\exp(-\Delta E/k_B T) \quad (22)$$

here, N_c is the conduction band density of state.

Thermal behavior of the voids affects the temperature characteristic (T_0) as shown in Fig. 5. It has been shown that the increase of the leakage current reduces T_0 [20].

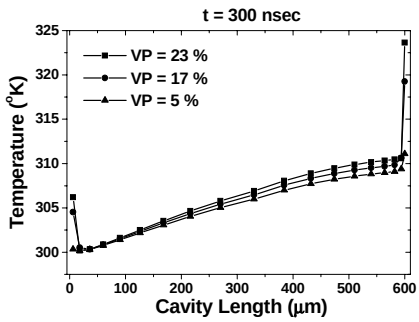

Fig. 3. Effects of voids on the temperature profile

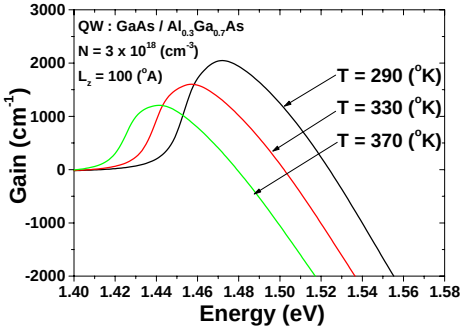

Fig. 4. Temperature dependence of the QW-laser gain

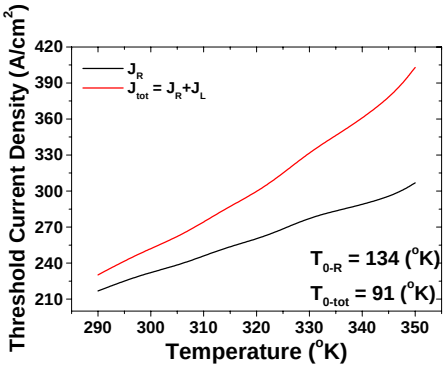

Fig. 5. Thermal effects on leakage and threshold currents, and temperature characteristic

In Fig. 6, the continuous wave (CW) mode *L-I* curve of the SQW-HPLD is plotted. The *L-I* curve for the mounted laser with no void at the interface, shows a smaller thermal rollover effect and a greater reliability, whereas in a mounted laser with 80% voided area the output power will show a greater instability as a result of poor heat sinking. This effect is in reasonable agreement with the experimental results [21].

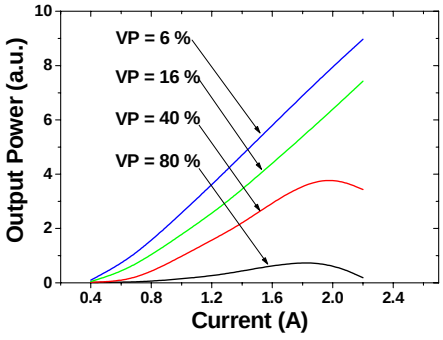

Fig. 6. Thermal effects of voids on the output power

ACKNOWLEDGEMENT

The authors would like to thank M. H. Yavari and M. Razaghi for their helpful comments.

V. Conclusion

This paper presents an exact model to simulate the void-induced thermal behavior of the HPLDs through a self-consistent solution of the rate equations coupled with the heat conduction equation. Voids in the die-attach solder interface can cause local hot spots which would degrade the optical performance of the laser. The 1-D model developed in this paper gives a good overall average junction temperature prediction including the effects of degraded die-attach. Using finite deference analysis, this result is improved by adding the effects of die-attach voids and hot spots on one-dimensional heat flow. The effects of voids on the threshold and leakage currents as well as on the laser's output power have been taken into account. Thermal mode hopping is also analyzed numerically. A full knowledge of the exact temperature profile along the cavity is an advantage in designing heat sinks capable of reducing COD for HPLDs.

References

[1] S. A. Merritt, P. J. S. Heim, S. H. Cho, and M. Dagenais, "Controlled solder interdiffusion for high power semiconductor laser diode die bonding,"*IEEE Trans. Comp. Pack. Manufact. Technol.*, part: B, vol. 20, No. 2, pp. 141-145, 1997.

[2] G. M. Smith, G. Yang, M. K. Davis, S. D. Solimine, R. Bhat, W. Liu, D. A. S. Loeber, F. Yang, A. Kussmaul, M. H. Hu, X. S. Liu, and C. E. Zah, "Design, performance, and reliability of 980 nm pump lasers," *Proceedings of the 16th Annual Meeting of the IEEE Lasers and Electro-Optics Society,* Vol. 1, pp. 417-418, 2003.

[3] D. A. Cohen, and L. A. Coldren, "Passive temperature compensation of uncooled GaInAsP-InP diode lasers using thermal stress," *IEEE J. Select. Topics Quantum Electron.*, vol. 3, no. 2, pp. 649-658, 1997.

[4] R. P. Sarzala, and W. Nakwaski, "Finite-element thermal model for buried-heterostructure diode lasers," *Opt. Quantum Electron.*, vol. 26**,** pp. 87–95, 1994.

[5] G. Berger, R. Muller, A. Klehr, and M. Voss, "Polarization bistability in strained ridge-waveguide InGaAsP/InP lasers: experiment and theory," *J. Appl. Phys.,* vol. 77, pp. 6135–44, 1995.

[6] R. Ait-Sadi, A. J. Lowery, and B. Tuck, "Two-dimensional temperature modelling of DH laser diodes using the transmission-line modelling (TLM) method," *IEE Proc. Sci. Meas. Techno*l., vol. 141, pp. 7–14, 1994.

[7] C. H. Henry, P. M. Petroff, R. A. Logan, and F. R. Merritt, "Catastrophic damage of $Al_xGa_{1-x}As$ double-heterostructure laser material," *J. Appl. Phys.*, vol. 50, pp. 3721–32, 1979.

[8] W. Nakwaski, "Three-dimensional time-dependent thermal model of catastrophic mirror damage in stripe-geometry double-heterostructure GaAs/(AlGa)As diode lasers," *Opt. Quantum Electron.,* vol. 21, pp. 331–4, 1988.

[9] G. Chen, and C. L. Tien, "Facet heating of quantum well lasers," *J. Appl. Phys.,* vol. 74, pp. 2167–74, 1993.

[10] A. J. Yerman, J. F. Burgess, R. O. Carlson, and C. A. Neugebauer, "Hot spots caused by voids and cracks in the chip mountdown medium in power semiconductor packaging," *IEEE Trans. Comp. Hybrid. Manufact. Technol.*, vol. CHMT-6, No. 4, pp. 473-479, 1983.

[11] N. Zhu, "Thermal impact of solder voids in the electronic packaging of power devices," *Proc. 15th Annu. IEEE SEMI-THERMAL Symp.*, San Diego, CA, pp. 22-29, 1999.

[12] X. Liu, K. Song, R. W. Davis, M. H. Hu, and C. E. Zah, "Design and implementation of metallization structures for epi-down bonded high power semiconductor lasers," *Proc. IEEE Elec. Comp. Technol. Conf.*, Corning, NY, pp. 798-806, 2004.

[13] H. C. Casey, and M. B. Panish, *Heterostructure Lasers*, Academic Press, New York, 1978.

[14] P. S. Zory, *Quantum Well Lasers*, Academic Press, 1993.

[15] S. R. Chinn, P. S. Zory, and A. R. Reisinger, "A model for GRIN-SCH-SQW diode lasers," *IEEE J. Quantum Electron.*, vol. 24, pp. 2191-214, 1988.

[16] G. P. Agrawal, and N. K. Dutta, *Semiconductor Lasers*, Van Nostrand Reinhold, New York, second edition, 1993.

[17] G. Tan, N. Bewtra, K. Lee, and J. M. Xu, "A two-dimensional nonisothermal finite element simulation of laser diodes," *IEEE J. Quantum Electron.*, vol. 29, pp. 822-35, 1993.

[18] W. W. Fang, C. G. Bethea, Y. K. Chen, and S. L. Chuang, "Longitudinal spatial inhomogeneities in high-power semiconductor lasers," *IEEE J. Select. Topics Quantum Electron.*, vol. 1, no. 2, pp. 117-28, 1995.

[19] S. Slivken, J. S. Yu, A. Evans, J. David, L. Doris, and M. Razeghi, "Ridge-width dependence on high-temperature continuous-wave quantum-cascade laser operation," *IEEE Photon. Technol. Lett.*, vol. 16, No. 3, pp. 744-746, 2004.

[20] N. K. Dutta, "Temperature dependence of threshold current of GaAs quantum well lasers," *Electron. Lett.*, vol. 18, pp. 451-453, 1982.

[21] M. H. Hu, X. Liu, C. Caneau, Y. Li, R. Bhat, K. Song, and C. E. Zah, "Testing of high power semiconductor laser bars," *J. Lightwave Technol.*, vol. 23, No. 2, pp. 573-581, 2005.